

NMR Imaging of Sea Spray Icing and Ice Adhesion Tests of Pliable Polymer Sheets for Deicing

T. Ozeki¹⁾, R. Yamamoto²⁾, S. Adachi³⁾ and K. Kose³⁾

¹⁾ Hokkaido University of Education

Iwamizawa 068-8642, JAPAN, oze@iwa.hokkyodai.ac.jp

²⁾ Hokkaido Kitami Ryokuryo High School

Kitami 090-8558, JAPAN, ray1982@hokkaido-c.ed.jp

³⁾ Institute of Applied Physics, University of Tsukuba

Tsukuba 305-8573, JAPAN, adachi@mrlab.frsc.tsukuba.ac.jp

Abstract— We have developed a compact NMR imaging system set up in a cold room to measure the three-dimensional microstructure of sea-spray icing. The presence of a channelized network of brine was confirmed in all sea spray icing samples in nature. The adhesion strength of ice on all test materials except fluoroethylene plastics decreased as the temperature increased above -10 °C. The difference between the fresh water adhesion strength of waterproofed nylons, polyurethane, and fluoroethylene plastics was small; these values were almost half or less as compared to that of stainless steel. Superhydrophilic plastic exhibited a higher strength than the other polymer sheets; however, the strength decreased to almost zero in the presence of salinity. The field test was conducted using two dummy lighthouses set up on the breakwater. Several types of membrane models were tested for wrapping the dummy lighthouses. Ice accretion often occurred on the lighthouse without the wrapped membrane, and icing was observed during half the observation period. On the other hand, the development of thick icing on the membrane was rare, although the top part of the lighthouse and the silicone sealant were often covered by ice. The icing period of the membrane revealed a significant difference as compared to the icing period without membrane; it is evident that the pliable sheets controlled the growth of icing. There was no significant difference between the water-repellent material and the hydrophilic material.

I. INTRODUCTION

THE northwestern coast of Hokkaido Island is characterized by heavy weather and extreme sea spray icing in winter. Heavy icing on lighthouses severely affects their maintenance in the northern harbors that face the Sea of Japan. One solution is to build sufficiently tall lighthouses that are more than 10 m in height; such lighthouses were conventionally used in Hokkaido. However, in recent years, these conventional lighthouses have been replaced by smaller and economical lighthouses. These small lighthouses were initially not equipped with countermeasures for spray icing. Their deicing is necessary in order to maintain their visibility; however, it is still a manual operation that typically involves the use of a hammer.

Several laboratory experiments have been performed to study the adhesion strength of saline ice and sea spray ice because the adhesion of saline ice to offshore structures is an

important issue (e.g., [1]–[3]). Field tests have also been performed (e.g., [4]–[6]). However, the measurement methods and results were different for each test. Recent studies have investigated the physical properties of sea spray ice. [7] measured the weight of ice and brine as well as the density, salinity, and growth rate of spray ice on a ship. He also measured the cross section of the accreted ice structure. [8] studied the microstructural features of spray ice on a ship and revealed a channelized network of brine. [9] reviewed a wet growth model of atmospheric icing on a structure. [10] simulated marine ice accretion using RIGICE04. On the other hand, icing tests using a canvas cloth were carried out in a laboratory experiment [11]. The cloths were coated with polypropylene, vinylidene fluoride, vinyl chloride, and silicone. However, these cloths were not practically used in the deicing of lighthouses. [12] performed laboratory experiments of saline ice adhesion on several chemical cloths. They obtained a preliminary result stating that deicing could be easily performed by vibrating the cloths.

In this research, we investigated the structural features of sea spray icing by using NMR imaging, and we then tested pliable sheets that can wrap the lighthouse. Adhesion strength tests of fresh ice and saline ice on polymer films and fabric materials were performed at various temperatures in a cold laboratory and in the field.

II. NMR IMAGING OF SEA SPRAY ICING

Brine pockets trapped in spray-ice matrices during wet growth are one of the structural features of sea-spray icing, while brine drainage control is one of the physical properties of spray ice. [13] designed an NMR imaging system to measure the 3D microstructure of sea-spray icing. It comprised a 4.74-T superconducting magnet and a specimen-cooling system that was controlled by adjusting the volume of cold airflow. However, the system was set up at room temperature and therefore temperature control of the ice sample was difficult. In order to address this problem, we have developed a compact NMR imaging system set up in a cold room to maintain the sample at a constant temperature.

The system comprises a permanent magnet, a gradient coil

set, and an RF probe installed in a cold room at a temperature of -5°C , as shown in Fig. 1. A compact MRI console was set up at room temperature beside the cold room. The permanent magnet is a yokeless magnet with a field strength of 1.04 T and weight of 300 kg.

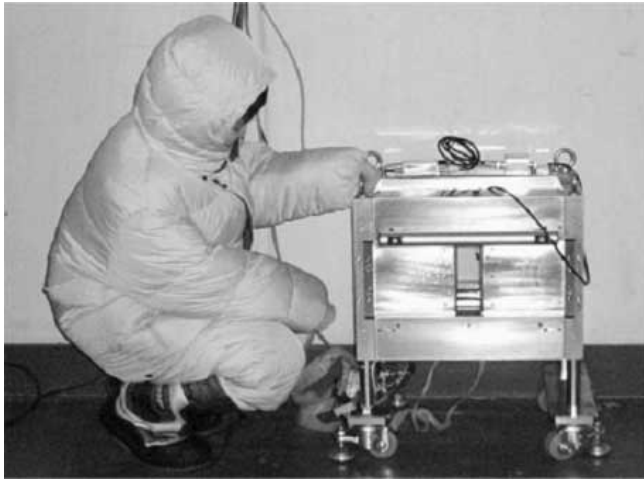


Fig. 1. The compact MRI system for cold room. Size = 45 cm (W) \times 38 cm (D) \times 58 cm (H).

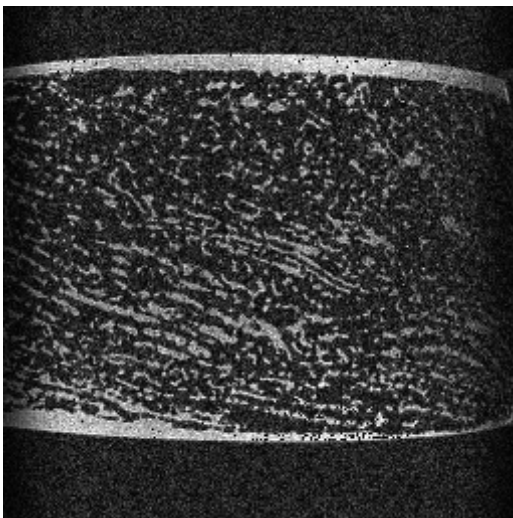


Fig. 2. A cross-sectional image of the sea-spray icing acquired from the 3D-DESE sequence. TR = 200 ms; TE = 8 ms; NEX = 4; image matrix size = 256 \times 256; pixel size = (123 μm)².

We obtained sea spray icing samples from the ice accretion on a lighthouse on the west coast of Hokkaido, Japan. Since the brine in the spray ice had drained out, we used a suction pump to fill the air gaps in the drainage channels with dodecane ($\text{C}_{12}\text{H}_{26}$). The signal from dodecane was sufficient to detect the location of the drainage channels.

A three-dimensional driven equilibrium spin-echo (3D-DESE) sequence (image matrix = 256³, voxel size = (123 μm)³) was used for 3D high-resolution imaging [14]. Fig. 2 shows a 2D slice selected from the 3D image data set. Since the NMR signal from the ice was negligible as compared to that from dodecane, the drainage channels appeared as bright regions. We also used maximum intensity projection (MIP) to visualize the drainage channels. Fig. 3 shows MIP views of

the vertical cross section of spray ice. The thickness is 1.2 mm. It indicates that sea spray icing has a developed network structure of drainage channels.

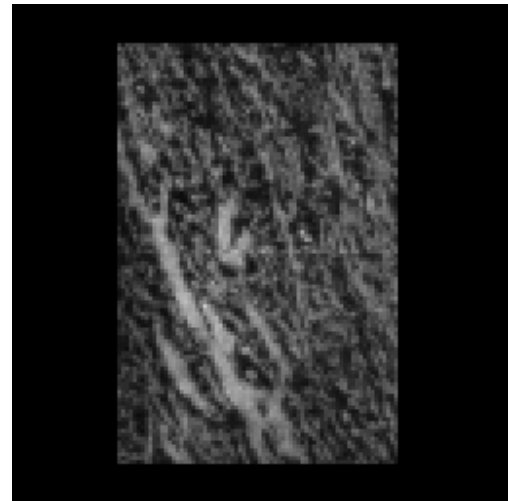


Fig. 3. MIP view of sea spray ice. Image matrix size = 128 \times 128; Thickness = 12 mm; pixel size = (200 μm)².

A channelized network of brine was confirmed in all sea spray icing samples in nature. On the other hand, there was no drainage channel in wet growth ice accretion by atmospheric icing. The channelized network of brine might be caused by the growth mechanism of sea spray ice.

III. ADHESION STRENGTH TEST OF POLYMER MATERIALS

A laboratory test was conducted in order to investigate the adhesion strength of fresh/saline ice on polymer materials. The experiments were performed using several materials. The test materials are listed in Table 1. The average roughness Ra is given by

$$Ra = \frac{1}{l} \int_0^l |Z(x)| dx \quad (1)$$

where $Z(x)$ is the height at x and l is the measurement length. Rz indicates the distance between the highest and lowest points in the measurement range. In this study, the fabric was required to possess the anti-icing feature as well as movability. The following six properties were considered in the selection of the test materials:

- (a) Ice adhesion strength,
- (b) Movability,
- (c) Tensile strength,
- (d) Weatherability,
- (e) Salinity tolerance, and
- (f) Cost.

Stainless steel was used in several laboratory experiments that investigated the adhesion strength of ice; hence, they were selected for comparisons with the results from earlier researches on this topic.

A schematic view of the apparatus is shown in Fig. 4. In this test, each test material was pasted on each of the stainless steel plates having a length and width of 60 mm; therefore, the material was not deformed although it comprised a cloth or a

film. The surface of the test piece was cleaned with a neutral detergent and fresh water. Water at 2 °C was poured into a 25-mm-diameter ring placed on the test piece, and ice was slowly frozen to reach the test temperature. When the test samples were completely frozen, they were maintained at the same temperature for another 2 h; the plate was then set on the testing device. The ice was removed from the plate by shearing with a pulling speed of 7 mm/min; a failure occurred within 3 s.

TABLE 1.
TEST SPECIMEN

	Materials	Roughness (μm)	
		Ra	Rz
Synthetic textiles	Waterproof nylon cloth	10.9	71.5
	Polyester coated with polyurethane (PE side)	17.0	162.3
	Polyester coated with polyurethane (PU side)	2.6	19.6
	Polyester without coating	8.5	81.5
Polymer films	Fluoroethylene plastic	0.3	1.4
	Super-hydrophilic plastic	0.3	1.7
Metal	Stainless steel	4.3	49.4

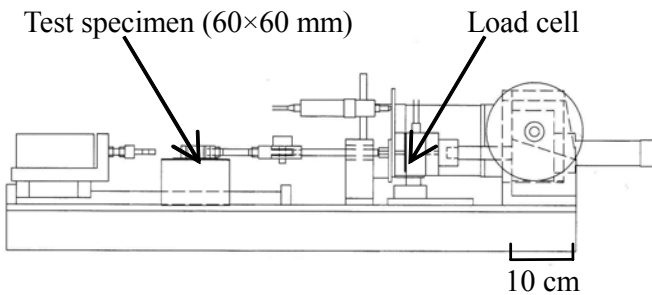


Fig. 4. A schematic view of the apparatus.

A. Temperature Dependence

The temperature dependence of the adhesion strength of ice was investigated using fresh ice. The air temperature in the cold room was maintained at -5 °C, -10 °C, -20 °C, and -25 °C. The results of the synthetic textiles are shown in Fig. 5. Each marker indicates the average value. The gray area indicates the values for stainless steel, and the width represents the standard deviation.

Nylon cloth, which was coated with acrylic resin for waterproofing, exhibited low adhesion strength at -5 °C and -10 °C, although the adhesion strength increased with a decrease in temperature. Two types of polyester cloths were used in this test. The adhesion strength of the polyester cloth was similar to that of stainless steel in the temperature range used in this test. Except for the result at -20 °C, there was no significant difference between the two polyester cloths, although the polyester cloth without coating was woven using a finer yarn; the roughness of this cloth was approximately

half of that of the other cloth. On the other hand, the coated polyester cloth exhibited low adhesion strength in all the temperature ranges. The polyurethane coating not only had low adhesion but was also waterproof and had a reduced roughness.

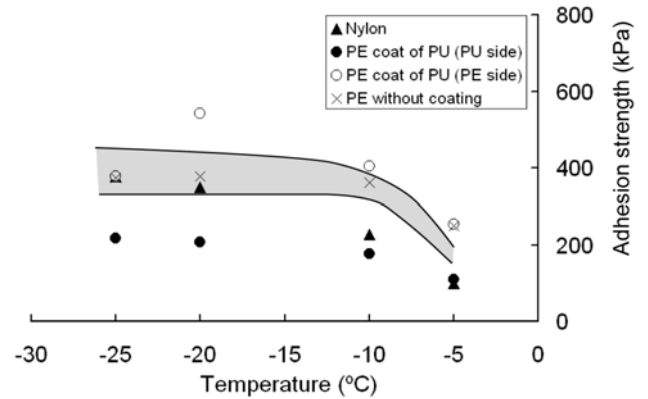


Fig. 5. Adhesion strengths of synthetic textiles. Gray area indicates the values for stainless steel.

The results of the polymer films are shown in Fig. 6. Each marker indicates the average value, and the error bar represents the standard deviation. The gray area indicates the values for stainless steel, and the width represents the standard deviation. Fluoroethylene plastic (ETFE) exhibited low adhesion strength (< 200 kPa) in all the temperature ranges. The adhesion strength of superhydrophilic plastic, which contains titanium oxide, exhibited a value similar to that of stainless steel in the temperature range used in this test. It can be summarized that the adhesion strength of ice on all test materials except ETFE decreased as the temperature increased above -10 °C, which was frequently encountered in this field test.

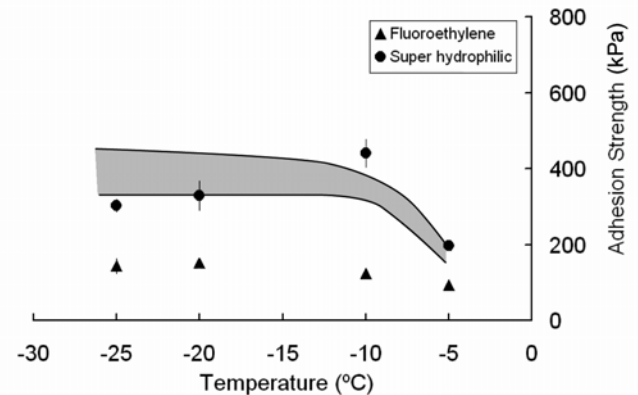


Fig. 6. Adhesion strengths of polymer films.

B. Adhesion Strength of Saline Ice

The adhesion strength of saline ice on the test materials was investigated at -20 °C. The test samples were prepared from water with salinities of 1‰, 3‰, 5‰, 10‰, 20‰, and 30‰. At salinities greater than 10‰, no adhesion was observed except in the polyester cloth because the brine

remained between the saline ice and the specimen.

The results corresponding to salinities of 1‰–5‰ are shown in Fig. 7. Each marker indicates the average value, and the error bar represents the standard deviation. For all the test materials, the adhesion strength decreases very rapidly as the salinity increases. This tendency was similar to that observed in stainless steel and other paints used in a previous research [3]. The ETFE film exhibited low adhesion strength in all the temperature ranges used in this test. The adhesion strength of the superhydrophilic film decreased remarkably with an increase in the salinity. This can be attributed to the superhydrophilic characteristics of the film that can satisfactorily maintain the brine between the saline ice and the specimen.

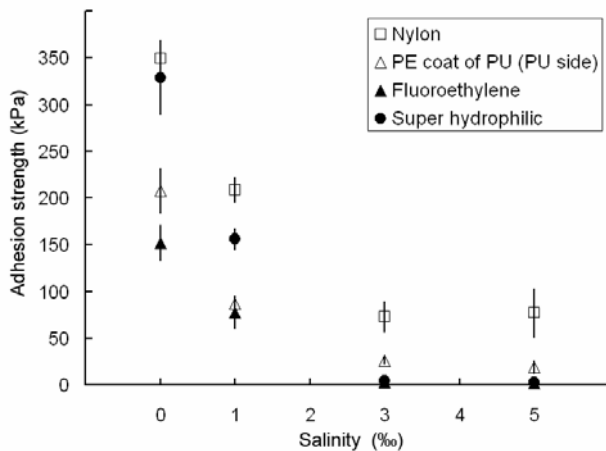


Fig. 7. Adhesion strength of saline ice. Temperature is -20°C .

IV. FIELD TEST

A. Site and Instruments

The field test was conducted at the Hamamasu harbor located on the west coast of Hokkaido during two winters (2004–2005 and 2005–2006). Two dummy lighthouses were set up on a breakwater extending from the north to the south: one was made of FRP and the other was made of steel coated with acrylic silicon resin. The height of both the dummy lighthouses was approximately 4 m.

Several types of membrane models, which were made of a cloth and a spacer, were tested for wrapping the dummy lighthouses. A spacer was installed between the dummy lighthouse and the membrane in order to facilitate the deformation of the cloth. Since ice is expected to exfoliate easily from the cloth due to fluttering, the membrane undergoes rapid distortion.

The FRP lighthouse was wrapped with a membrane model coated with polytetrafluoroethylene during the winter of 2004–2005. During the winter of 2005–2006, the FRP lighthouse was tested without the membrane. On the other hand, for the steel lighthouse, the superhydrophilic film model was tested during the two winter periods. A superhydrophilic film was pasted on a polyester cloth. The ice accretion on the

dummy lighthouses was recorded by a monitoring system.



Fig. 8. Sea spray icing on dummy steel lighthouse.

B. Anti-icing Feature

In this test, icing occurred on the windward side or the top part of the lighthouse during all the icing events. Fig. 8 shows the ice accretion on the steel dummy lighthouse; the superhydrophilic membrane was wrapped around the bottom half of the lighthouse. From this figure, it is evident that the membrane structure controls the growth of icing. Fig. 9 shows a telephotograph recorded by the monitoring system on January 25, 2006. Sea spray ice was observed on the windward side (left) of the FRP lighthouse. Ice accretion often occurred on the dummy lighthouse without a wrapped membrane. On the other hand, the icing on the membrane tended to be partial, e.g., icing was observed on the top part of the lighthouse or the silicone sealant part. Table 2 lists the number of times icing occurred during the two winters. The tables also list the total number of days in which icing was observed during the test period. The result indicates that ice/snow accretion on the lighthouse without the wrapped membrane was observed during almost half of the observation period. By using the membrane models, the total number of days during which icing was observed reduced by approximately five times. Significance tests (level of significance $\alpha = 0.05$) indicated that there were obvious significant differences between the steel lighthouse and the polytetrafluoroethylene model, and between the FRP lighthouse and the superhydrophilic film model as well.

It can be concluded that deicing was easy for the membrane models due to the low adhesion strength and the vibration or exfoliation caused by strong winds and green water. In the case of sea spray ice, the superhydrophilic membrane models worked favorably because of the low adhesion strength of saline ice. When the membrane was coated with thick icing, the cloth could not undergo fluttering or distortion, and deicing was difficult. For example, the top part of the membrane model was flat; therefore, ice accretion occurred in the form of crown snow and the icing gradually grew downward.

TABLE 2.
TIMES AND TOTAL DAYS OF ICING FOR 2004–2006 WINTER

	Number of times	Icing days
Steel (coated with acrylic silicone resin)	5	33/63
FRP	4	30/67
Polytetrafluoroethylene	2	7/63
Super-hydrophilic film	1	5/89

(2004-2005 winter: 63 days, 2005-2006 winter: 67 days)



Fig. 9. FRP (left) and wrapped (right) lighthouses on Jan. 25, 2006.

V. CONCLUSIONS

In order to visualize the brine pockets trapped in spray-ice

matrices, we developed a compact NMR imaging system set up in a cold room to maintain the sample at a constant temperature. Since the brine in the spray ice had drained out, we used a suction pump to fill the air gaps in the drainage channels with dodecane ($C_{12}H_{26}$). The presence of a developed network structure of drainage channels was confirmed in all sea spray icing samples in nature. It indicates that brine entrapped in sea spray icing drains out by the channels, and some portion of the brine may reach the boundary between the icing and the base structure.

In order to decrease the sea spray icing on small lighthouses on a breakwater, we designed pliable sheets that wrap the lighthouse. The membrane structure was made of a chemical cloth and a spongy spacer. The features of icing on the sheets and the deicing conditions were verified by cold experiments conducted in the laboratory and field.

An adhesion strength test was carried out using several test materials at various temperatures. The adhesion strength of ice on all test materials except ETFE decreased as the temperature increased above $-10\text{ }^{\circ}\text{C}$. The difference between the fresh water adhesion strength of waterproofed nylons, polyurethane, and ETFE was small; these values were almost half or less as compared to that of stainless steel. Superhydrophilic plastic exhibited a higher strength than the other polymer sheets; however, the value decreased drastically with a little salinity.

The field test was conducted using two dummy lighthouses set up on the breakwater. Several types of membrane models were tested for wrapping the dummy lighthouses. Ice accretion often occurred on lighthouses without the wrapped membrane, and icing was observed during half the observation period. On the other hand, the development of thick icing on the membrane was rare, although the top part of the lighthouse and the silicone sealant were often covered by ice.

It is evident that the pliable sheets controlled the growth of icing. However, certain problems were encountered during the practical implementation of this membrane model; these problems must be resolved. A balance between pliability and durability is very important for the membrane because pliability generally decreases with an increase in durability. The pasted film and polyurethane coating on the cloth could not withstand the fluttering and green water through one entire winter, resulting in their breakage. Further tests are required in order to decide which material is more effective for the deicing of sea spray ice—a water-repellent material or a hydrophilic material. Countermeasures to deal with icing around the floodlight are a subject for future work.

VI. ACKNOWLEDGMENT

We are grateful to the Ocean Policy Research Foundation for supporting this research. We express our gratitude to Dr. H. Kitagawa of the Ocean Policy Research Foundation and Dr. L. Makkonen of the Technical Research Center of Finland for their useful comments and discussions. We are also grateful to N. Yamamoto, K. Ishizuka, and T. Satou of the Japan Coast Guard for their support in the field observations. We also

thank S. Handa of the University of Tsukuba and Dr. T. Haishi of MR Technology for their assistance in operating the NMR imaging system. Part of this research was supported by a scientific research fund from the Ministry of Education, Culture, Sports, Science and Technology of Japan.

VII. REFERENCES

- [1] N. S. Stehle, "Adfreezing strength of ice," in *Proc. International Symposium on Ice*, Paper 5.3., p. 13, 1970.
- [2] J. L. Laforte and L. Lavigne, "Microstructure and mechanical properties of ice accretions grown from supercooled water droplets containing NaCl in solution," in *Proc. 3rd International Workshop on Atmospheric Icing of Structures*, Paper 3.4., p. 5, 1986.
- [3] L. Makkonen and E. Lehmus, "Studies on adhesion strength of saline ice," in *Proc. 9th International Conference on Port and Ocean Engineering under Arctic Conditions*, pp.45–55, 1987.
- [4] W. M. Sackinger and P. A. Sackinger, "Shear strength of the adfreeze bond of sea ice to structures," in *Proc. 4th International Conference Port and Ocean Engineering under Arctic Conditions*, pp.607–614, 1977.
- [5] H. Saeki, T. Ono and A. Ozaki, "Mechanical properties of adhesion strength of ice to pile structures," in *Proc. International Symposium on Ice*, 2, pp.641–649, 1982.
- [6] H. Saeki, T. Ono, T. Takeuchi, S. Kanei and N. Nakazawa, "Ice forces due to changes in water level and adfreeze bond strength between sea ice and carious materials," in *Proc. 5th Offshore Mechanics and Arctic Engineering Conference*, 4, pp.534–540, 1986.
- [7] N. Ono, "Studies on the ice accumulation on ships. 2. On the conditions for the formation of ice and the rate of icing," *Low Temperature Science*, A22, pp.171–181, 1964. [in Japanese with English summary]
- [8] C. C. Ryerson and A. J. Gow, "Crystalline structure and physical properties of ship superstructure spray ice," *The Royal Society Physical Transactions*, A358, pp.2847–2871, Nov. 2000.
- [9] L. Makkonen, "Models for the growth of rime, glaze, icicles and wet snow on structures," *The Royal Society Physical Transactions*, A358, pp.2913–2939, Nov. 2000.
- [10] T. W. Forest, E. P. Lozowski and R. Gagnon, "Estimating marine icing on offshore structures using RIGICE04," in *Proc. 11th International Workshop on Atmospheric Icing of Structures*, p. 8, 2005.
- [11] Japan Aids to Navigation Association, "Kouro-hyoushiki-kinou ni eikyou wo oyobosu koori no jokyo-taisaku ni kansuru tyousa-kenkyu," Research Report, p. 53, 1986. [in Japanese]
- [12] T. Ozeki, H. Kitagawa, K. Izumiyama, H. Shimoda and K. Kosugi, "An investigation of sea spray icing and deicing on membrane structures," in *Proc. 11th International Workshop on Atmospheric Icing of Structures*, p. 4, 2005.
- [13] T. Ozeki, K. Kose, T. Haishi, S. Nakatsubo and Y. Matsuda, "Network images of drainage channels in sea spray icing by MR microscopy," *Magnetic Resonance Imaging*, 23, pp.333–335, 2005.
- [14] N. Iita, S. Handa, S. Tomiha and K. Kose, "Development of a compact MRI system for measuring the trabecular bone microstructure of the finger," *Magnetic Resonance in Medicine*, 57, pp.272–277, 2007.